Specific heat of C_{60} and K_3C_{60} thin films for $T=6-400$ K

K. Allen and F. Hellman
Department of Physics, University of California, San Diego, California 92093
(Received 13 January 1999; revised manuscript received 14 May 1999)

Using a microcalorimeter, we have measured the specific heat of C_{60} and K_3C_{60} thin films from 6–400 K. The results can be understood by analyzing the phonon modes; the electronic specific heat of K_3C_{60} is a small fraction of the total. While C_{60} displays a clear separation of energy levels between interball and intraball modes, the added (alkali) optical modes in K_3C_{60} blur this separation because they appear in the gap. Additionally, the acoustic modes of K_3C_{60} soften compared to pure C_{60}. [S0163-1829(99)01039-5]

I. INTRODUCTION

C_{60} was discovered in 1985 (Ref. 1) and has been widely available since 1991.[2] Shortly thereafter it was found that K_3C_{60} is a metal and a superconductor,[3] with the surprisingly high transition temperature of 19 K. This marked the beginning of a full-blown research effort to understand all kinds of fullerenes, with particular emphasis on alkali-intercalated C_{60} materials.

Pure C_{60} draws research interest as a novel molecular solid because the molecular units are so large and symmetric. Structural and bonding issues are of primary importance, not only intrinsically but also in their effects on electronic properties. The A_3C_{60} materials are interesting because they are not conventional metals, as numerous experiments have shown. The most striking evidence for atypical behavior comes from the nonsaturation of the resistivity with temperature.[4] Both K_3C_{60} and Rb_3C_{60} have room-temperature resistivity near 1.5 $m\Omega\,cm$, four times larger than the Ioffe-Regel limit, implying a mean free path shorter than the intermolecular spacing. As the temperature increases up to 800 K, the resistivity never levels off, rising beyond the point where the mean free path is shorter than even the interatomic spacing. Thus, the simple Drude formula for mean free path is inappropriate for these materials.

In addition, the weak bonding and consequently large distance between the cages results in a narrow [$\approx$0.5 eV (Ref. 5)] conduction band, nearly an order of magnitude smaller than for conventional metals. The low electron density in K_3C_{60} [4×10^{21} cm^{-3} (Ref. 6)] implies poor screening. Numerous theoretical models and experiments show a large electron correlation energy, on the order of 1.0–1.8 eV,[7] meaning that electron-electron interactions are strong. The transport properties of K_3C_{60} are strongly affected by such unconventionality; for instance, this material can be driven from superconducting to insulating solely by the addition of disorder, extremely rare for a three-dimensional system.[8]

All of these factors indicate the anomalous electronic properties of A_3C_{60}, but in addition, there are important questions of bonding. Pure C_{60} has only weak van der Waals bonds between the neutral balls; K_3C_{60} has K^+ ions filling the spaces between $C_{60}{}^{3-}$ molecules, so that the interaction is primarily ionic. The structure and lattice constant of C_{60} and K_3C_{60} are nearly the same. One can ask how the presence of the K between the C_{60} molecules affects the phonon spectrum.

Some of the questions about these materials can be addressed through heat-capacity measurements. There have been many previous specific-heat studies of pure C_{60} (Refs. 9–14) and K_3C_{60} (Ref. 15). Despite some initial confusion due to differences in sample quality, the vibrational modes and bonding in pure C_{60} have been well understood through C_p measurements, as we will describe in detail in Sec. III A. Our pure C_{60} results are fully consistent with past studies.

Because K_3C_{60} is a metal and a superconductor, one would like to learn from C_p measurements the value of γ, the coefficient of the electronic specific heat ($C_{\text{electronic}}=\gamma T$), which is proportional to the density of electronic states at the Fermi level $N(\epsilon_F)$, as well as the value of the discontinuity in C_p at the superconducting transition. Beyond metallic properties, heat capacity can reveal how strongly the lattice specific heat is affected by the changes in intermolecular potential from the different bonding in C_{60} and K_3C_{60}. The only previous measurement of the specific heat of K_3C_{60} (Ref. 15) addresses the first two electronic issues (as discussed in Sec. III B), but not the lattice properties.

Our experiments show that phonons and localized lattice excitations strongly dominate the specific heat at temperatures from 6 to 400 K. Due to the small electronic heat capacity, no information about the electronic term could be extracted. Therefore, we focus on drawing conclusions about the phonon density of states (DOS) and the bonding in C_{60} and K_3C_{60}.

The lattice specific heat is related to the phonon density of states in energy space $D(\omega)$ through

$$C_{\text{lattice}}(T)=k_B\int_0^\infty \frac{x^2e^x}{(e^x-1)^2}D(\omega)\,d\omega, \tag{1}$$

where $x=\hbar\omega/k_BT$ and k_B is the Boltzmann constant.[16] We compare our C_p results to those obtained by integrating a published DOS (Ref. 17) from neutron scattering results. For the C_{60}, the specific heat obtained from the published DOS matches our measured results moderately well, but for K_3C_{60}, the match is quite poor. We then work backward from our data to construct a crude model of the difference in DOS between C_{60} and K_3C_{60}, illuminating the essential

physics: C_{60} shows a clear separation of energy regimes in the DOS between low-energy interball modes and high-energy intraball (on-ball) modes, while in K_3C_{60} the separation is blurred due to the addition of alkali optical modes in the gap. Additionally, below 140 K—a temperature regime dominated completely by the acoustic phonon modes—the specific heat of K_3C_{60} is larger than that of C_{60}, showing that the acoustic modes of K_3C_{60} are softer than those of pure C_{60}.

II. EXPERIMENTAL DETAILS

A. Measurement method

The specific heat was measured with our thin-film calorimeter devices, which have been described in detail elsewhere.[18] Briefly, the device consists of an 1800-Å amorphous SiN membrane, which serves to thermally isolate the sample, surrounded by a Si frame. A thin-film Pt heater and three thin-film thermometers cross the membrane, and each thermometer has an identical matching partner on the frame. One thermometer is Pt, working in the range 40 K–800 K; the other two are different geometries of amorphous Nb_8Si_{92}, together spanning the range 1 K–300 K. A metallic conduction layer is deposited on the center of the backside of the device so that it is in thermal, but not electrical, contact with the electronics on the front. This layer assures that the thermally isolated features on the membrane come to equilibrium among themselves much more quickly than any applied heat can leak back to the Cu block. The sample also goes on the backside, on top of the conduction layer. The sample and conduction layer are deposited through a shadow mask that sits less than 25 μm from the membrane surface to give a well-defined area.

The measurement is made using the standard relaxation method.[19] Solving the heat-flow equation for this device yields the result $C=\kappa\tau$, where C is the heat capacity of everything in direct thermal contact with the conduction layer (sample, membrane electronics, a patch of membrane, the conduction layer itself); κ is the thermal conductance of the leads and membrane that provide the heat link between the sample and the Si frame, which is thermally grounded to the cryostat block; and τ is the characteristic time for the heat to leak from sample to block. τ and κ are measured by a standard ac bridge technique. The heat capacity of the thermometers, heater, membrane, and conduction layer (known as the addenda) were measured before depositing the sample. This addenda is then subtracted from the subsequently measured total heat capacity, which includes the sample. It accounts for 30–80% of the total heat capacity and was subtracted as a smooth curve.

The mass of the sample must also be measured in order to convert heat capacity (J/K) to specific heat (J/g K). The sample area was well known from the size of the shadow mask, and the thickness was determined by a crystal monitor located near the sample during deposition. The bulk density was used to calculate the mass, an assumption later justified for the pure C_{60} by comparing our measured specific heat to literature values. It is likely that the K_3C_{60} sample also had the bulk density because it was made by intercalating potassium into an already-deposited C_{60} film. For pure C_{60}, we have also checked the thickness by placing a blank substrate near the device during deposition, then measuring the film thickness directly on a profilometer after removal from the chamber. This method cannot be used for K_3C_{60} because the film immediately reacts with air, causing the potassium to migrate to the surface and form potassium oxides and the C_{60} lattice to relax.

B. Sample deposition

The samples were deposited onto devices already containing a conduction layer of 2500 Å of polycrystalline gold, evaporated at ambient temperature in a separate chamber. X-ray diffraction experiments that we performed on a C_{60} film grown on polycrystalline gold under somewhat different deposition conditions (0.2 Å/sec, 180 °C) showed a grain size of 4200 Å. Thus, we expect this sample had smaller grains.

The C_{60} and K_3C_{60} were evaporated from thermal sources in an ultrahigh vacuum (UHV) deposition chamber, which contains three thermal evaporation sources and a liquid-nitrogen-cooled shroud to reduce the deposition pressure. Under the conditions used in the present work, the pressure of the chamber prior to evaporation is 5×10^{-10} torr. The C_{60} source was sublimed powder from MER Corporation loaded into a baffled tungsten boat, while the potassium was grown from getter sources from SAES Inc. Both the C_{60} and the K (when used) were thoroughly outgassed before deposition. The substrate temperature during deposition was 135 °C; the pressure during deposition was 3×10^{-8} torr. In the case of pure C_{60}, we used a deposition rate of 1 Å/sec, growing the film to 7000-Å thick (mass 7.4 μg).

Growing the best K_3C_{60} film required balancing the competing factors of grain size, deposition rate, and alkali intercalation. A compromise between these considerations led to the following growth scheme: The 4500-Å K_3C_{60} film (5.5 μg) was grown in three separate sequential steps, each 1500-Å thick (i.e., 1500 Å of pure C_{60} was grown and then potassium was intercalated into it, three times in a row). The deposition rates were 0.2 Å/sec for C_{60} and 0.1 Å/sec for K. For each 1500-Å step, the four-wire resistance of the film was monitored using a SiN substrate with prepatterned contacts. The K was deposited until the film reached a resistivity minimum, which corresponds to K_3C_{60}.[20] Then the next layer was grown in a similar fashion. The resistance of the film after the second layer did not drop by a full factor of 2 compared to the first layer, which we take as evidence that the second and third C_{60} layers had smaller grains than the first due to potassium from the lower layer(s) diffusing into the fresh C_{60}. The film grown by this method showed resisitivity characteristics similar to those seen in single crystals. It had positive (''metallic'') slope at high temperatures, low room-temperature resistivity for K_3C_{60} (2.5 mΩ cm), a high superconducting onset temperature (19.2 K), and a relatively narrow superconducting transition (2 K) (see Fig. 1).

C. Cryostats

Due to the great air sensitivity of K_3C_{60}, all measurements on this material must be performed *in situ* or on samples otherwise sealed from oxygen exposure. We measured the heat capacity of the K_3C_{60} sample *in situ* using a ^{4}He cryostat mounted on top of the UHV deposition system,

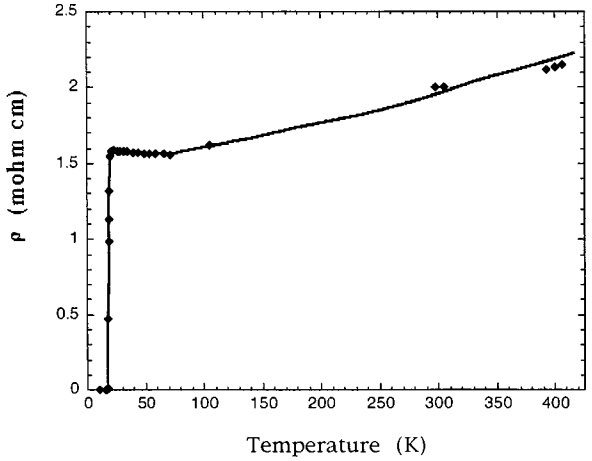

FIG. 1. Resistivity of K_3C_{60} sample, 4500 Å, substrate temperature during deposition 135 °C. The substrate was *a*-SiN covered by 2500 Å polycrystalline gold. This sample was grown simultaneously with the heat-capacity sample, next to the C_p device.

with a cold finger which extends into the chamber. This cryostat has been constructed with UHV-compatible materials (for example, high-melting-temperature solder was used and vacuum grease was not). Its temperature range of operation is 2.5 K to 500 K; other details have been published previously.[8]

The calorimeter device with the less air-sensitive pure C_{60} was removed from the deposition chamber and measured *ex situ* in two systems. The low-temperature cryostat, designed by RMC (now Desert Cryogenics), has a standard copper cold finger and radiation shield, and a brass vacuum attached by a greased taper seal. The temperature range of operation is 1.5–310 K. For the high-temperature C_{60} data (300–400 K), a different *ex situ* setup was used, which has been described previously.[21]

III. RESULTS AND DISCUSSION: C_{60} AND K_3C_{60}

Figure 2 shows the specific heat of C_{60} and K_3C_{60} as a function of temperature in units of J/g K. Both these units and J/mol K have conceptual advantages and disadvantages for these materials. Comparing units, numbers of modes, and the density of states for C_{60} and K_3C_{60} is subtle; the details are worked out explicitly in the Appendix. For convenience in this text, we will treat the units of J/g K as primary; to convert to J/mol K, where a mole refers to carbon atoms for C_{60} and average atoms for K_3C_{60}, multiply the C_{60} data by 12 and the K_3C_{60} data by 13.3. For moles of molecules, multiply the per gram results by 720 for C_{60} and 837 for K_3C_{60}.

A. Pure C_{60}: Separation of energy levels

Our C_{60} measurement covers the widest temperature range for a clean (sublimed) sample. A number of earlier results over smaller ranges or with lower quality samples have been published in the literature,[9–14] and we note that our data match well with previous results.

The first-order orientational transition is clearly visible near 250 K. Using $S=\int(C/T)\,dT$ and $H=\int C\,dT$, we found the changes in entropy ΔS and enthalpy ΔH at the transition

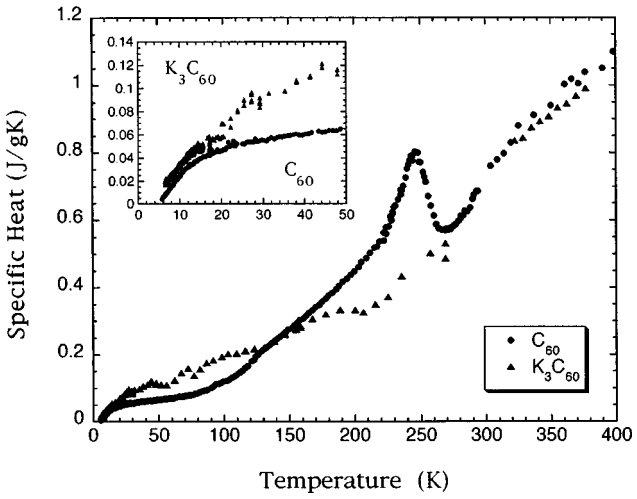

FIG. 2. Specific heat of C_{60} and K_3C_{60}. For the C_{60}, the lower plateau corresponds to the saturation of intermolecular modes; with three translational (acoustic) and three librational modes, the saturation value is 69.3 mJ/g K. The equivalent saturation for K_3C_{60} (i.e., all modes not on the ball) is 150 mJ/g K. The saturation values for the total DOS are 2.08 J/g K (C_{60}) and 1.88 J/g K (K_3C_{60}), which are not reached at the temperatures shown. Note that the specific heat of K_3C_{60} exceeds that of C_{60} from 6–140 K, and on a molar plot (J/mol K), this difference is further enhanced (details of the Dulong-Petit limits and conversion to molar quantities are worked out in the appendix). Inset: an expanded view of the region below 50 K.

from our data by measuring the excess specific heat above a smooth background through 250 K: 30.5 J/g K and 6.67 J/g, respectively. These values are in good agreement with model calculations[22] (26.5 J/g K and 6.7 J/g), as well as previous experimental results[23] (41.7 J/g K and 5.9 J/g).

The overall shape of the C_{60} specific-heat curve can be understood in the following way, as articulated by Olson *et al.*[13] Note that there is an initial rise in the specific heat, followed by a plateau near 80 K, then another steep, nearly linear rise. This two-tiered behavior corresponds to a *separation of energy levels* in the phonon spectrum. The low-energy excitations are translations and rotations (also called librations) involving the entire C_{60} cage. Because the bonds between cages are weak van der Waals bonds, these low-energy modes saturate below 80 K. With six modes (three translational and three librational) and a molecular number density ($N/60$), the Dulong-Petit limit for the C_{60} *molecules* is $6(N/60)k_B = 69.3$ mJ/g K, which matches the level of the plateau. Calculations[24] and measurements[25] of the speeds of sound in C_{60} give a Debye temperature of about 90–100 K, reasonably consistent with this saturation occurring near 80 K in our data.

Above the temperature where the low-energy modes saturate, the higher-energy excitations *on* the ball start to be activated and contribute to the specific heat, causing the sharp rise above 100 K. The Dulong-Petit limit for the carbon *atoms* is equal to $3Nk_B = 2.08$ J/g K. The saturation temperature is not reached in our experiment or any other published specific-heat results; based on the highest-energy on-ball mode (196 meV),[26] this temperature is expected to be above 2500 K. (Since C_{60} sublimes around 300 °C, it could not be observed anyway.) It is the large difference in bond strength

between the covalent bonds on the cage and the molecular bonds between the cages that leads to the separation of energies in the phonon spectrum.

We note briefly that the roughly linear dependence of C_p above 100 K corresponds to a broad, nearly constant density of phonon states, which arises from the multitude of on-ball modes (see Sec. III C).

Looking in more detail, we consider the low-temperature behavior of C_p. In the Debye model, the T^3 regime can be expected no higher than about 1/10 the saturation temperature, and a common rule of thumb (accounting for deviations from the Debye model) is 1/50. From the data, we see that the intermolecular modes of C_{60} saturate near 80 K, and therefore the T^3 regime for the specific heat is not expected above 8 K and could occur below 2 K. Recall also that the intermolecular modes consist of both acoustic (translational) modes and librations. There is no reason to assume that these two kinds of excitations have the same saturation temperature; therefore, the shape of the C_p curve below 80 K may be non-Debye-like even if both kinds of modes are well described by Debye functions. Indeed, Beyermann, Hundley, and Thompson[10] have analyzed their specific-heat data in the regime 1–20 K, and they find that a sum of two Einstein terms, a Debye term, and a linear term is required to accurately model the data. Our data are nearly identical to theirs in the overlapping region (6–20 K). Therefore, there is no true low-temperature ''Debye regime'' above 6 K in which the excitations are in the long-wavelength continuum limit.

A low-temperature T^3 behavior in C_p arises from a phonon density of states $D(\omega)$ that varies as ω^2. The lack of a T^3 regime implies that the DOS does not vary as ω^2 until below the energy corresponding to 6 K [$=0.52$ meV/$\hbar$].

B. K_3C_{60}: Small electronic term

Figure 2 shows our measurement of the specific heat of K_3C_{60} compared to that of C_{60}. We first note that K_3C_{60} shows no orientational transition below 400 K associated with the breaking of spherical symmetry when the balls stop rotating freely, consistent with NMR experiments.[27] The presence of the potassium hinders rotation. The balls sit in one of two inequivalent orientations, which is called ''merohedral disorder,'' at all temperatures relevant to this study.[26]

We now turn to the analysis of the electronic contribution to the specific heat: the value of γ and the jump at T_c. The first has only been measured indirectly, and the second only measured once. The relevant experiments were performed by Ramirez *et al.*[15] and Burkhart and Meingust.[28] Ramirez *et al.* measured the heat capacity of a thick film of K_3C_{60} deposited on the inside of a quartz ampoule from 4–25 K. Using the jump in the specific heat at T_c and information about the superconducting parameters from other experiments, Ramirez *et al.* calculated a value for γ: 3.1×10^{-5} J/g K^2. Burkhart and Meingust measured the volume expansion coefficient of K_3C_{60} pellets, from which γ can also be calculated; they found 3.7×10^{-5} J/g K^2. For comparison, a typical metal has γ about an order of magnitude smaller.[29] The large value in K_3C_{60} is due to a high density of electronic states $N(E_f)$, which results from the narrow conduction band.

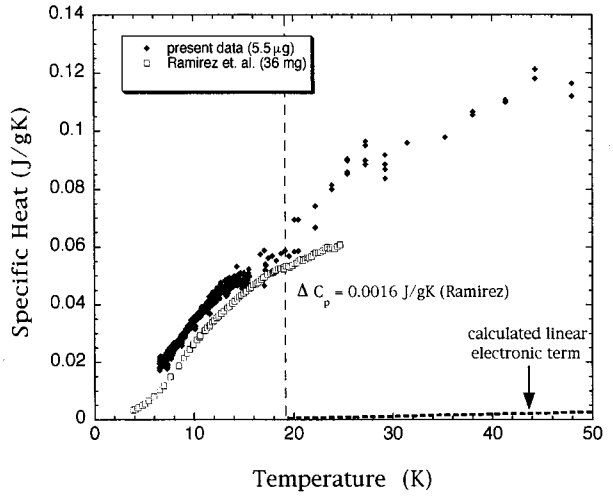

FIG. 3. Low-temperature portion of K_3C_{60} specific heat.

The electronic term associated with the average calculated γ value (3.4×10^{-5} J/g K^2) is plotted in Fig. 3, along with the low-temperature portion of our K_3C_{60} data and Ramirez' results, which span the range 4–25 K. We see that even below 50 K, the electronic contribution to the total specific heat of K_3C_{60} is small; it is even smaller at higher temperatures. The superconducting transition is at 19 K, and below T_c, the electronic heat capacity drops exponentially[16] and is even less of the total.

The dashed vertical line in Fig. 3 represents T_c, the superconducting transition temperature. By plotting their data on a log-log scale, Ramirez *et al.* find an experimental value of $\Delta C=1.6$ mJ/g K. Using the calculated γ of 3.1×10^{-5} J/g K^2, $C_{\text{electronic}}$ at T_c is 5.89×10^{-4} J/g K, so that the ratio of ΔC to $C_{\text{electronic}}$ at T_c is 2.72, somewhat higher than the predicted BCS value of 1.43 (Ref. 16) (this has been interpreted as strong electron-phonon coupling in fullerene superconductors). Going the other way, Burkhart's γ of 3.7×10^{-5} J/g K^2 in conjunction with these values for the ratio gives a jump in the specific heat of 1–2 mJ/g K. These values for the jump are below the level of the noise in our data, and indeed, we see no evidence of a jump, so it was not possible for us to estimate ΔC.

It is clear from Fig. 3 that the specific heat of K_3C_{60} is dominated by nonelectronic terms to which we now turn.

C. Blurred energy levels and the density of states

Figure 2 shows that in K_3C_{60}, unlike C_{60}, there is no clear saturation of low-energy modes and no plateau in C_p. As determined in the Appendix, the saturation value for all modes not on the ball in K_3C_{60} is 150 mJ/g K. There is a slight flattening in $C_p(T)$ near this value, but not as distinct as in the case of C_{60}.

The differences between C_p in C_{60} and K_3C_{60} can be explained by the changes in the acoustic modes due to the K ions, as well as the appearance of new alkali optical modes. Some of the modified modes are very soft, contributing weight at the lowest energies, which accounts for K_3C_{60}'s larger specific heat at low temperature, while the alkali optical modes appear in the gap between interball and intraball modes[26] and cause the blurring of the separation.

For K_3C_{60}, the charge transfer is nearly complete,[30] so the crystal consists of K^+ and C_{60}^{3-} ions, giving K_3C_{60} a different intermolecular potential than that of the neutral molecular solid C_{60}. It is not clear what the effect on the phonons will be: On the one hand, ionic bonds should stiffen the lattice because the attraction of the charged units exceeds the attraction of the induced dipoles of van der Waals bonds, and steric hindrance could possibly play a stiffening role also. On the other hand, metallic screening tends to soften the phonons. Raman and IR spectroscopy indicate that most shifts in on-ball modes between C_{60} and K_3C_{60} are small ($\leqslant$ a few percent).[31] Further, neutron studies show that the repulsive part of the A-C_{60} potential is as important as the Coulombic part in determining the orientational potential.[32] Note from Fig. 2 that the specific heat of K_3C_{60} exceeds that of C_{60} from ~6–140 K, indicating that the low-energy intermolecular modes shift to lower energy, and therefore these cannot be the source of the lack of C_p plateau and blurred energy levels.

To examine the phonon density of states in these materials more carefully, we first compared our specific-heat data to published neutron-scattering results. The DOS (Ref. 33) can be calculated from neutron-scattering results, combined with appropriate force constants known from theory.[34] Gompf *et al.*[17] have done this for C_{60} and K_3C_{60} using a model based on strong (covalent) nearest-neighbor interactions on the C_{60} molecules and weak van der Waals or weak ionic interactions between balls.

Using this calculated DOS for both C_{60} and K_3C_{60}, we have done the integral in Eq. (1) to determine the corresponding C_{lattice} in the range 1–400 K. (As a check, we also did the calculation up to 3500 K and confirmed that it approached the correct Dulong-Petit limit in each case.) The results are shown in Figs. 4 and 5, along with our own model which will be described shortly. For C_{60}, the calculated C_{lattice} has the correct qualitative two-tiered shape but does not quantitavely match the data at low temperature, due either to inaccuracy of the low-energy neutron data or to incorrect mode counting in the model used to convert the neutron data to a DOS. For K_3C_{60}, the problems are more serious; the calculated C_{lattice} does not even qualitatively match the blurred shape of the K_3C_{60} C_p data. First, it retains the two-tiered shape because too few modes appear in the gap to blur the separation of energy levels. Also, there is too little weight at the lowest energies; K_3C_{60}'s greater specific heat below 140 K requires the interball modes to become even softer than they are in pure C_{60}. (More detailed information about this comparison to neutron results can be found in Ref. 35.)

Using a different neutron scattering technique, Neumann *et al.*[32] focused their studies on the low-energy regime ($\leqslant$10 meV) in C_{60}, K_3C_{60}, and other fullerenes. Since they were primarily interested in the orientational potential of these materials, they did not calculate a phonon DOS, but some of their findings can be compared with our specific heat results. In particular, they find significant neutron-scattering intensity near 2.5 meV in C_{60}, which is due to the very soft librational modes. This is very close to the librational energy we found to best match our specific-heat results, as described below. However, Neumann's results indicate that in K_3C_{60} the acoustic modes are stiffer than those in C_{60} (peaked near 4 meV), while we found that they had to be slightly softer to account for the larger C_p in K_3C_{60} at low temperature.

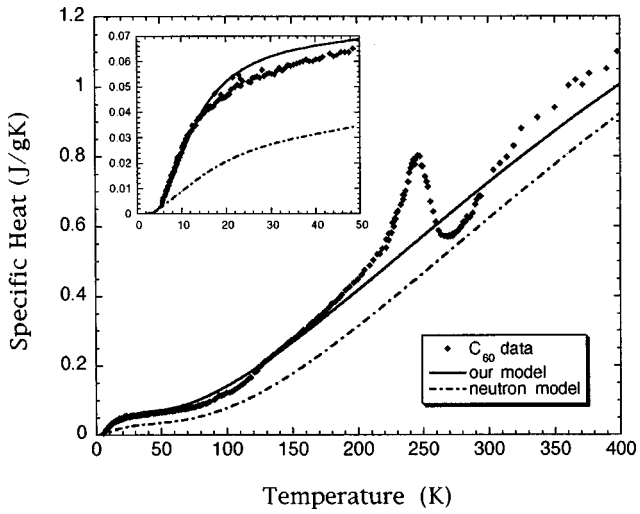

FIG. 4. Our C_{60} data compared to our model (Fig. 6) and to the specific heat calculated [using Eq. (1)] from the published neutron DOS (Ref. 17). Neither our model nor the neutron result is expected to display the orientational peak because no provision was made in the calculations for the number of modes to change with temperature. Inset: The region below 50 K.

To understand more clearly how the differences between the specific heats of C_{60} and K_3C_{60} result from differences in the DOS, we constructed two crude model densities of states, based on knowledge of the relative weights of different modes (see the Appendix). We have confirmed that they approach the correct Dulong-Petit limits at high temperature: 2.08 J/g K for C_{60} and 1.88 for K_3C_{60}. The models are shown in Fig. 6. The simple rectangular shapes are fairly accurate in the case of C_{60}, which has many excitations of similar energy,[26] but less accurate for K_3C_{60}. (Note that at the lowest energy, the true DOS must drop as E^2 in the elastic limit, so this simple model will not produce a specific heat that approaches zero correctly at the lowest temperature.)

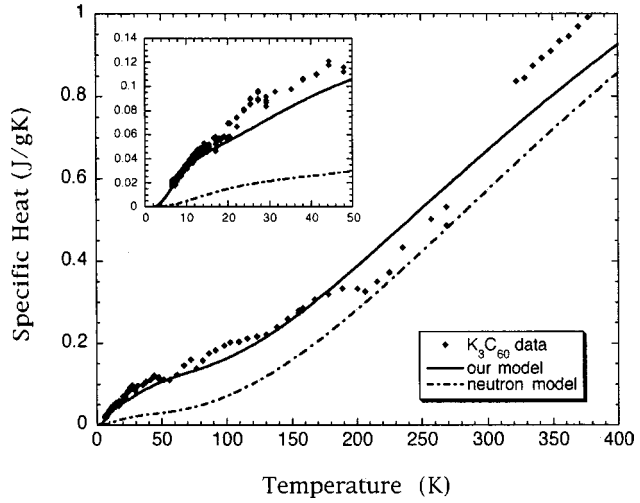

FIG. 5. Our K_3C_{60} data compared to our model (Fig. 6) and to the specific heat calculated [using Eq. (1)] from the published neutron DOS (Ref. 17). Inset: The region below 50 K.

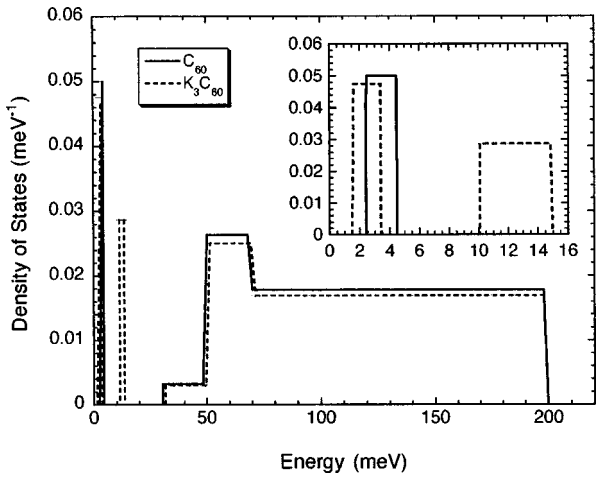

FIG. 6. Model densities of states for C_{60} and K_3C_{60}. The solid line model represents C_{60}, with a well-defined separation of energy levels. The dashed line model simulates the case of K_3C_{60}, with weight shifted to lower energies and states in the gap. The states at the lowest energy ($\leqslant$5 meV) are associated with acoustic modes, the large blocks at high energy ($\geqslant$30 meV) with the numerous on-ball modes, and the peak between 10–15 meV with the optical modes of K_3C_{60}. The integrated DOS under each block was constrained to match the number of modes of each type (see the Appendix for details). Both models were tuned to produce C_p curves that resemble our experimental results. Inset: The low-energy region. The real DOS must approach 0 as E^2; this has no impact on C_p in the measured temperature range.

For C_{60}, we chose two regions separated by a gap, indicative of the separation of energy levels. To obtain the correct C_p shape in the range 100–200 K, it was necessary to add some structure to the intraball phonons, with less weight from 30–50 meV and more from 50–70 meV. The resultant specific heat is shown in Fig. 4 along with our C_{60} data. Note that this sort of model is not expected to reproduce the orientational peak in the specific heat because that peak occurs when the number of phonon modes abruptly changes at 250 K. The overall match between our model and the data is excellent, including the initial rise at low temperature.

In the case of K_3C_{60}, some weight is shifted to even lower energies to reproduce the greater magnitude of the K_3C_{60} specific heat over the C_{60} specific heat. Note that if the data were plotted as J/mol K instead of J/g K the difference at low temperature would be further enhanced, because K_3C_{60} has larger mass per mole than C_{60}. We also added alkali optical modes in the gap to blur the separation of energy levels. The specific heat calculated from this model is compared to our K_3C_{60} data in Fig. 5. The match is again quite good for such a simple model.

IV. CONCLUSIONS

In summary, our specific-heat measurements (6–400 K) indicate that the lattice contribution dominates C_p in K_3C_{60} and that C_{60} and K_3C_{60} have significantly different densities of phonon states. Pure C_{60} exhibits a separation of energy levels in its DOS due to differing bond strengths on and between molecules, which results in a two-tiered shape to the specific heat as the intermolecular modes saturate before the on-ball modes become excited. The intermolecular modes are very soft, so that there is no T^3 dependence to C_p down to at least 6 K. In K_3C_{60}, the separation of energy levels is blurred so that the two-tiered behavior is not evident.

Using published densities of states for C_{60} and K_3C_{60} calculated from neutron results to determine the specific heat, we find a consistent qualitative picture for the case of C_{60}: the modes are separated into two regimes. But for K_3C_{60}, too few modes are added at low temperature and in the gap, so the model does not match the specific-heat data. More significant changes are needed to give K_3C_{60} a higher specific heat at low temperature and to eliminate the two-tiered shape of C_p.

Our own simple model densities of states, constructed to resemble our specific-heat results upon integration, show that adding alkali optical states in the gap and at the lowest energies accounts well for the differences in specific heat between C_{60} and K_3C_{60}.

APPENDIX: MODE-COUNTING AND THE DENSITY OF STATES IN C_{60} AND K_3C_{60}

Enumerating the vibrational modes in these materials can become confusing, especially when translating between gram and molar quantities. In this appendix, we explicitly count the nonelectronic modes contributing to the specific heat of C_{60} and K_3C_{60}, divide these into low- and high-energy portions, and calculate the weights of these modes in the densities of states.

C_{60} is a pure material, so it is unambiguous to consider the density of states per *atom* (of carbon). We write this as

$$D(E) = \frac{\text{number of modes}}{\text{eV (carbon atom)}}. \tag{A1}$$

Since the total number of modes is $3N$, where N is the number of carbon atoms, the area under $D(E)$ is constrained:

$$\int_0^\infty D(E)\, dE = 3. \tag{A2}$$

Each unit cell contains 60 carbon atoms. Therefore, there are 180 total modes of vibration in this material. Recalling that C_{60} displays a separation of energy levels between low-energy interball modes and high-energy on-ball modes, it makes sense to divide these modes into two categories: the first consisting of rotations of the entire ball, called librations (three modes), plus acoustic phonons (three modes), and the second consisting of on-ball modes. Thus, the interball modes account for 6 out of 180 modes, and the on-ball modes are the remaining 174. Integrating just the area of the DOS under the interball modes should give a value $3 \times \frac{6}{180} = 0.1$. The remaining 2.9 is the area under the on-ball modes, and a gap separates these two regions of the DOS.

The Dulong-Petit limit is 25 J/mol K. Since a mole of carbon atoms has mass 12 g (i.e., a carbon atom weighs 12 amu), this limit becomes 2.08 J/g K for C_{60}. (*Caveat*: the orientational transition at 250 K slightly changes this result, as described in the paragraph below. However, the small change does not affect the analysis in this paper.) Since the interball modes account for 6/180 total modes, the saturation value for the interball modes is 1/30 of 2.08 = 69 mJ/g K.

As a brief aside, it is worth noting the effect of the orientational transition at 250 K in pure C_{60} on the specific heat. Above this transition, the balls spin freely, which means that there is no potential energy associated with their rotational motion (because there is no restoring force). Recall that in the classical, high-temperature limit, each squared term in the Hamiltonian (called a *degree of freedom*) contributes $1/2k_B$ to the heat capacity per atom, so that usually a set of three modes will contribute $3k_B$, with three kinetic and three potential degrees of freedom. However, the three rotational modes in C_{60} do not contribute the full $3(N/60)k_B$ to the specific heat above 250 K; they only contribute $3/2(N/60)k_B$. Thus, the true Dulong-Petit limit is $3Nk_B - (3/2)(N/60)k_B = 119Nk_B/40 = 24.79$ J/mol K $= 2.07$ J/g K instead of 2.08. This does not change any of our conclusions, and for convenience, we will treat the high-temperature Dulong-Petit limit as $3Nk_B$.

Moving on to the case of K_3C_{60} at high temperature, we now must consider an *average atom* occupying the unit cell, which contains three potassium atoms and 60 carbon atoms. This average atom has mass $[(3)(39)+(60)(12)]/63 = 13.3$ amu. The density of states is now expressed as:

$$D'(E) = \frac{\text{number of modes}}{\text{eV (average atom)}}. \tag{A3}$$

Equation (A2) is still true for $D'(E)$—it just refers to the modes of the average atoms. The total area is still 3.

Dividing up the modes is somewhat more difficult. Consider all the modes that are *not* high-energy (on-ball) modes. This amounts to considering the C_{60} molecule as a large ''atom''—in other words, conceptually the material is K_3X, with four ''atoms'' per primitive unit cell. We consider an fcc structure, ignoring the orientation of the balls because it does not affect the mode counting result. There are a total of 12 modes $(=4\times3)$, of which 3 are acoustic. Therefore, nine are optical. We still must add in the three rotational modes that we counted above for the case of C_{60}. This makes a total of 15 modes not on the ball. The remaining 174 are the on-ball modes (the same number as we found in the case of C_{60}).

Since there are now 63 average atoms per unit cell, there are 189 total modes, which are distributed in the ratios derived in the previous paragraph. This makes the relative weights of the portions of the DOS slightly different: the acoustic and rotational modes have total area $3\times\frac{6}{189} = 0.095$; the optical modes $3\times\frac{9}{189} = 0.143$. Thus, the total weight of non-on-ball modes is 0.24 in K_3C_{60} (within rounding). The on-ball modes have weight $3\times\frac{174}{189} = 2.76$. Note that the total is still 3.

In terms of moles of *average* atoms, the Dulong-Petit limit is still 25 J/mol K. Since an average atom weighs 13.3 amu, this limit for K_3C_{60} translates to 1.88 J/g K. Although the modes do not clearly separate in this material (recall Fig. 2), we can derive a theoretical saturation value for the modes that are not on the ball. Since these modes account for 15 out of 189 total modes, they should saturate at $1.88\times\frac{15}{189} = 150$ mJ/g K.

It is worth noting finally how to conceptualize the difference between $D(E)$ for C_{60}, which is expressed in terms of carbon atoms, and $D'(E)$ for K_3C_{60}, which is expressed in terms of average atoms. We can write

$$\frac{\text{modes}}{\text{eV (carbon atom)}} = \frac{\text{modes}}{\text{eV (average atom)}}\,\frac{\text{number of average atoms}}{\text{number of carbon atoms}}, \tag{A4}$$

where there are 63 average atoms per 60 carbon atoms. Therefore, we can understand why the on-ball modes have different weights in $D(E)$ and $D'(E)$—their weight in the case of C_{60} (2.9) is equal to their weight in the case of K_3C_{60} (2.76) times the conversion factor $\frac{63}{60}$.

Expressing the C_p data in terms of J/g K is unambiguous in the sense that there is no question what a ''gram'' refers to; units of J/mol K must always be accompanied by a specification of the molar quantity (carbon atoms, C_{60} molecules, or average atoms). Thus, we have chosen to present the data in gram units, although they do carry the disadvantage of having different Dulong-Petit limits for different materials.

ACKNOWLEDGMENTS

We thank S. Watson, R. Dynes, D. Arovas, and J. Ostrick for valuable discussions and insights. This work was supported by NSF Grant No. DMR-9208599.

[1] H. W. Kroto, J. R. Heath, S. C. O'Brien, R. F. Curl, and R. E. Smalley, Nature (London) **318**, 62 (1985).

[2] W. Krätschmer, L. D. Lamb, K. Fostiropolous, and D. R. Huffman, Nature (London) **347**, 354 (1990).

[3] A. F. Hebard, M. J. Rosseinsky, R. C. Haddon, D. W. Murphy, S. H. Glarum, T. T. M. Palstra, A. P. Ramirez, and M. Kortan, Nature (London) **350**, 600 (1991).

[4] A. F. Hebard, T. T. M. Palstra, R. C. Haddon, and R. M. Fleming, Phys. Rev. B **48**, 9945 (1993).

[5] S. Saito and A. Oshiyama, Phys. Rev. Lett. **66**, 2637 (1991).

[6] K_3C_{60} is fcc with lattice constant 14.24 Å; three electrons per C_{60}; O. Zhou, G. B. M. Vaughan, Q. Zhu, J. E. Fischer, and P. A. Heiney, Science **255**, 833 (1992).

[7] See, for example, R. W. Lof, M. A. van Veenendaal, B. Koopmans, H. T. Jonkman, and G. A. Sawatsky, Phys. Rev. Lett. **68**, 3924 (1992); P. A. Brühwiler, A. J. Maxwell, A. Nilsson, and N. Martensson, Phys. Rev. B **48**, 18 296 (1992); J. H. Weaver, J. Phys. Chem. Solids **53**, 1433 (1992); S. Chakravarty and S. Kivelson, Europhys. Lett. **16**, 751 (1991).

[8] S. K. Watson, K. Allen, D. W. Denlinger, and F. Hellman, Phys. Rev. B **55**, 3866 (1997).

[9] T. T. T. Atake, H. Kawaji, K. Kikuchi, K. Saito, S. Suzuki, I. Ikemoto, and Y. Achiba, Physica C **185-189**, 427 (1991).

[10] W. P. Beyermann, M. F. Hundley, and J. D. Thompson, Phys. Rev. Lett. **68**, 2046 (1992).

[11] T. Matsuo, H. Suga, W. I. F. David, R. M. Ibberson, P. Bernier,

A. Zahab, C. Fabre, A. Rassat, and A. Dworkin, Solid State Commun. **83**, 7111 (1992).
[12] E. Grivei, B. Nysten, M. Cassart, A. Demain, and J.-P. Issi, Solid State Commun. **85**, 73 (1993).
[13] J. R. Olson, K. A. Topp, and R. O. Pohl, Science **259**, 1145 (1993).
[14] J. E. Fischer, A. R. McGhie, J. K. Estrada, M. Haluska, H. Kuzmany, and H.-U. ter Meer, Phys. Rev. B **53**, 11 418 (1996).
[15] A. P. Ramirez, M. J. Rosseinsky, D. W. Murphy, and R. C. Haddon, Phys. Rev. Lett. **69**, 1687 (1992).
[16] N. W. Ashcroft and D. N. Mermin, *Solid State Physics* (Saunders, Philadelphia, 1976).
[17] F. Gompf, B. Renker, H. Schober, P. Adelmann, and R. Heid, J. Supercond. **7**, 643 (1994).
[18] D. W. Denlinger, E. N. Abarra, K. Allen, P. W. Rooney, M. T. Messer, S. Watson, and F. Hellman, Rev. Sci. Instrum. **65**, 946 (1994).
[19] R. Bachmann, F. J. DiSalvo, T. H. Geballe, R. L. Greene, R. E. Howard, C. N. King, H. C. Kirsch, K. N. Lee, R. E. Schwall, H. U. Thomas, and R. B. Zubeck, Rev. Sci. Instrum. **43**, 205 (1972).
[20] G. P. Kochanski, A. F. Hebard, R. C. Haddon, and A. T. Fiory, Science **255**, 184 (1992).
[21] E. N. Abarra, Ph.D. thesis, University of California, San Diego, 1996.
[22] R. Saito, G. Dresselhaus, and M. S. Dresselhaus, Phys. Rev. B **49**, 2143 (1994).
[23] P. A. Heiney, J. Phys. Chem. Solids **53**, 1333 (1992).
[24] R. Venkatesh and R. V. G. Rao, Phys. Status Solidi B **201**, 361 (1997).
[25] N. P. Kobalev, R. K. Nicolaev, Y. M. Soifer, and S. S. Khasanov, Phys. Rev. B **46**, 12 737 (1992).
[26] M. S. Dresselhaus, G. Dresselhaus, and P. C. Eklund, *Science of Fullerenes and Carbon Nanotubes* (Academic Press, San Diego, 1996).
[27] S. E. Barrett and R. Tycko, Phys. Rev. Lett. **69**, 3754 (1992).
[28] G. J. Burkhart and C. Meingast, Phys. Rev. B **54**, R6865 (1996).
[29] C. Kittel, *Introduction to Solid State Physics* (Wiley, New York, 1996).
[30] R. M. Fleming, M. J. Rosseinsky, A. P. Ramirez, J. C. Tully, R. C. Haddon, T. Siegrist, R. Tycko, S. H. Glarum, P. Marsh, G. Dabbagh, S. M. Zahurak, A. V. Makhija, and C. Hampton, Nature (London) **352**, 701 (1991).
[31] M. S. Dresselhaus, G. Dresselhaus, and P. C. Eklund, J. Mater. Res. **8**, 2054 (1993).
[32] D. A. Neumann, J. R. D. Copley, D. Reznik, W. A. Kamitakahara, J. J. Rush, R. L. Paul, and R. M. Lindstrom, J. Phys. Chem. Solids **54**, 1699 (1993).
[33] The density of states from neutron results is often called the ''generalized density of states'' (GDOS) because the weights of the phonons are convoluted with the scattering power of each element making up the material. However, for pure or nearly pure materials like C_{60} and K_3C_{60}, the GDOS is essentially identical to the phonon density of states, and in this paper we ignore the difference.
[34] H. Schober, A. Tölle, B. Renker, R. Heid, and F. Gompf, Phys. Rev. B **56**, 5937 (1997).
[35] K. J. Allen, Ph.D. thesis, University of California, San Diego, 1998.